

See discussions, stats, and author profiles for this publication at: <https://www.researchgate.net/publication/239717664>

Electrosynthesis and Electrochemical Characterization of a Thin Phase of Cu_xS ($x \rightarrow 2$) on ITO Electrode

ARTICLE in *LANGMUIR* · OCTOBER 2002

Impact Factor: 4.46 · DOI: 10.1021/la025711k

CITATIONS

38

READS

33

9 AUTHORS, INCLUDING:



Ricardo Córdova

Pontificia Universidad Católica de Valparaíso

19 PUBLICATIONS 179 CITATIONS

SEE PROFILE



Humberto Gomez

Pontificia Universidad Católica de Valparaíso

102 PUBLICATIONS 1,611 CITATIONS

SEE PROFILE



Jose Ramos Barrado

University of Malaga

172 PUBLICATIONS 2,323 CITATIONS

SEE PROFILE



Rodrigo del Rio

Pontifical Catholic University of Chile

45 PUBLICATIONS 416 CITATIONS

SEE PROFILE

Electrosynthesis and Electrochemical Characterization of a Thin Phase of Cu_xS ($x \rightarrow 2$) on ITO Electrode

Ricardo Córdova,^{*,†} Humberto Gómez,[†] Ricardo Schrebler,[†] Paula Cury,[†]
Marco Orellana,[†] Paula Grez,[†] Dietmar Leinen,[‡]
José Ramón Ramos-Barrado,[‡] and Rodrigo Del Río[†]

Instituto de Química, Universidad Católica de Valparaíso, Avda. Brasil 2950, Valparaíso, Casilla 4059 Valparaíso, Chile, and Laboratorio de Materiales y Superficie, Unidad Asociada al CSIC, Departamento de Física Aplicada I, Departamento de Ingeniería Civil, Materiales y Fabricación, Universidad de Málaga, E29071, Málaga, Spain

Received March 8, 2002. In Final Form: August 21, 2002

Cu_xS ($x \rightarrow 2$) thin films were obtained by sulfidization of copper thin films previously obtained by spin-coating from a dichloromethane solution of $[\text{Cu}(\text{II})(2\text{-ethyl hexanoate})_2(\text{H}_2\text{O})_2]$ deposited on ITO substrate, irradiated with UV light and electrochemically reduced. Through cyclic voltammetry experiences performed in a 0.05 M $\text{Na}_2\text{B}_4\text{O}_7$ buffer solution containing 5 mM Na_2S , the electroformation mechanism of Cu_xS phase is controlled by a first electron transfer, obtaining an initial formation of $\text{Cu}(\text{HS})_{\text{ads}}$ that evolves to a Cu_xS phase. Potentiostatic current transient recorded in the potential range of $-0.8 \text{ V} \leq E \leq -0.7 \text{ V}$ showed that the nucleation and growth mechanism of the Cu_xS phase obeys a two-dimensional instantaneous process with diffusional and charge-transfer contributions. AFM analysis of the deposits shows that Cu_xS phase is preferentially deposited in the valleys left by ITO particles. The average size of Cu_xS particles is close to 20 nm. Cyclic voltammetry results, electromotive force determination in the $\text{Cu}/\text{Cu}_{\text{aq}}^{2+}/\text{Cu}_x\text{S}$ galvanic cell, EDAX, and UV analysis demonstrate that the stoichiometric factor x in Cu_xS is close to 2. The electro-obtained Cu_xS phase was unstable and evolved to other nonstoichiometric compounds at open circuit. The processes responsible for the instability were the own oxidation of Cu_xS phase and the water reduction that takes place over Cu_xS and bare ITO particles. The last process was studied by electrochemical impedance spectroscopy. Photoelectrochemical measurements in the stability potential range of the Cu_xS phase shows that the electro-obtained phase presents a p-type conductivity.

Introduction

Interest in the synthesis of a Cu_xS phase ($x \rightarrow 2$) has been largely due to its application in the $\text{Cu}_2\text{S}/\text{CdS}$ solar cells. This compound was considered as a precursor reagent in the anodic electrochemical synthesis of films of the ternary semiconductor compound CuInS_2 .¹ The Cu_xS films can be obtained by chemical or electrochemical methods. Studies concerning the electrodeposition of Cu_xS on polycrystalline copper electrodes in sulfide-containing solutions employing different electrochemical and optical characterization techniques have been previously published.^{1–6} A chemical synthesis of copper sulfide thin film has been realized by successive ionic layer adsorption and reaction method (SILAR).⁷

It is well-known that copper sulfides represented as Cu_xS ($x \rightarrow 2$) have distinct composition at room temperature due to the variation in the stoichiometric factor value

($1 \leq x \leq 2$). The copper–sulfur phase diagram shows four stable and distinct phases: chalcocite (Cu_2S), djurite ($\text{Cu}_{1.96}\text{S}$), annilite ($\text{Cu}_{1.75}\text{S}$), and covellite (CuS).⁸ The oxidation state of Cu_xS -type compounds increases from chalcocite to covellite, and the oxidation of these phases plays an important role in the change from one composition to another. During the anodic oxidation of a synthetic sample of Cu_2S , different intermediate phases have been identified by X-ray diffraction and reflectance spectra measurements.⁸ Besides, the copper sulfide composition has been determined from electromotive force measurements in the $\text{Cu}/\text{Cu}_{\text{aq}}^{2+}/\text{Cu}_x\text{S}$ galvanic cell, and the diffusion of copper in copper sulfide was studied as a function of x by electrochemical impedance spectroscopy (EIS).⁹ These experiments show that the value of the copper diffusion coefficient was dependent on the stoichiometry of the considered phase.

In general, Cu_xS ($x \rightarrow 2$) compounds exhibit a p-type semiconductor character with copper vacancy defect as acceptors. Also, it has been proved that the photo-voltametric behavior of a natural or synthetic chalcocite is dependent on the stoichiometry and that the photocurrent observed is lowered when the x value in Cu_xS ($x \rightarrow 2$) decrease.^{5,10} On the other hand, the absorption maxima spectra of copper sulfide shifts toward lower wavelengths with decreasing copper content, behavior that

[†] Universidad Católica de Valparaíso.

[‡] Universidad de Málaga.

* Corresponding author: e-mail rcordova@ucv.cl; phone + 56 32 273179; Fax +56 32 212746.

(1) Schimmel, M. I.; de Tacconi, N. R.; Rajeshwar, K. *J. Electroanal. Chem.* **1998**, *453*, 187.

(2) Vázquez Moll, D.; DeChialvo, M. R. G.; Salvarezza, R. C.; Arvia, A. *J. Electrochim. Acta* **1985**, *30*, 1011.

(3) Engelken, R. D.; McCloud, H. E. *J. Electrochem. Soc.* **1985**, *132*, 567.

(4) de Tacconi, N. R.; Rajeshwar, K.; Lezna, R. O. *J. Phys. Chem.* **1996**, *100*, 18234.

(5) Scharifker, B. R.; Rugeles, R.; Mosota, J. *Electrochim. Acta* **1984**, *29*, 261.

(6) Schimmel, M. I.; Bottechia, O. L.; Wendt, H. *J. Appl. Electrochem.* **1998**, *28*, 299.

(7) Sartale, S. D.; Lockhande, C. D. *Matter. Chem. Phys.* **2000**, *65*, 63.

(8) Koch, D. F. A.; McIntyre, R. J. *J. Electroanal. Chem.* **1976**, *71*, 285.

(9) Cassaignon, S.; Sánchez, S.; Guillemoles, J.-F.; Vedel, J.; Gómez Meier, H. *J. Electrochem. Soc.* **1999**, *146*, 4666.

(10) Gómez, H.; Vedel, J.; Córdova, R.; Schrebler, R.; Basáez, L. *J. Electroanal. Chem.* **1995**, *388*, 81.

has been attributed to a progressive lower Fermi level–conduction band edge gap when increasing from Cu_2S to CuS .⁶

Despite the interest showed for the study of the Cu_xS ($x \rightarrow 2$) phase, the electrochemical synthesis of thin or nanocrystalline films of this compound is scarce. Recently, the electrochemical synthesis of thin film of Cu_2S on titanium substrate were performed in an acid electrolytic solution containing Cu^{2+} , $\text{S}_2\text{O}_3^{2-}$, and EDTA ions. The films obtained were characterized by SEM and XRD.¹¹

The thickness and nanocrystallinity of semiconductor films are important aspects for the design of photoelectrochemical solar energy devices or photovoltaic treatment for hazardous wastes. The nanostructured film of semiconductors shows quantum-size effects which allow tailoring of the energy band structure and thus the properties of the semiconductor.¹²

The aim of this work is to study the electroformation of a thin film Cu_xS ($x \rightarrow 2$) phase on a copper film previously deposited on a ITO glass substrate by the spin-coating technique. This technique have demonstrated to be useful for the obtention of thin films of metal deposits.^{13,14} The electrochemical study was performed using cyclic voltammetry, cyclic photovoltammetry, potentiostatic current–time transients, and EIS techniques. The morphology of the Cu_xS ($x \rightarrow 2$) phase formed was studied by atomic force microscopy, and some evidence of its stoichiometry was obtained by EDAX and optical absorbance spectra.

Experimental Section

All electrochemical experiments were made in a single-compartment three-electrode cell at room temperature (20 °C) and under an inert atmosphere. A large area platinum wire was used as a counter electrode. The reference electrode used was an Ag/AgCl electrode ($E = 0.197$ V vs NHE). All measurements are referenced to this electrode. The working electrode consisted of ITO glass covered by a thin copper film.

The thin copper film on ITO was obtained through the following procedure: An ITO glass (Delta-Technologies Limited, $R_s \leq 10 \Omega$) ($7 \times 25 \times 0.9$ mm) was placed on a spin-coater apparatus and rotated at a speed of 2400 rpm. A portion (0.3 mL) of a solution (5 g L^{-1}) of the compound copper [Cu(II)(2-ethyl hexanoate)₂·(H_2O)₂] in dichloromethane was dispensed onto the ITO glass and allowed to spread. The motor was then stopped, and a thin film of the complex remained on the ITO glass substrate. Afterward, the sample was irradiated with light from a UV lamp (UVP, model UVS-28, 254 nm, 8 W) by 24 h. A film that contains a mixture of copper metal and oxygen containing copper species was obtained due to the photodecomposition of the organic complex.^{13,14} Subsequently, to reduce all oxygen-containing copper species, a potentiostatic pulse at -1.0 V during 20 min in a 0.05 M $\text{Na}_2\text{B}_4\text{O}_7$ buffer solution was applied to ITO substrate with an expose area of 1 cm^2 . This electrode (electrode A) was characterized by cyclic voltammetry in the potential range of -1.0 to 0 V at a scan rate of 0.02 V s^{-1} .

A voltammetric study of an electrode A in 0.05 M $\text{Na}_2\text{B}_4\text{O}_7$ buffer solution (pH 9.2) containing 10 $\text{mM} \geq \text{HS}^- \geq 0.1$ mM at scan rate 0.1 $\text{V s}^{-1} \geq v \geq 0.002$ V s^{-1} was performed. First, electrode A was polarized at -1.0 V for 10 min. Then, sodium sulfide solution was added while the polarization was maintained for 10 min. Then the cyclic voltammetry program was applied. The potential range in the positive going potential scan was -1.0 to -0.6 V and in the negative going potential scan was -0.6 to -1.2 V.

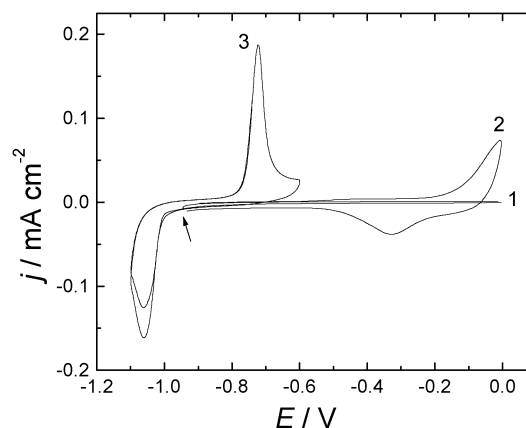


Figure 1. Cyclic voltammograms of different electrodes in 0.05 M $\text{Na}_2\text{B}_4\text{O}_7$ at 0.02 V s^{-1} : (1) ITO electrode; (2) electrode A in the absence of sodium sulfide; (3) electrode A in the presence of 5 mM Na_2S (anodic charge, $Q_a = 0.595$ mC cm^{-2}).

Potentiostatic current transients studies were carried out in 0.05 M $\text{Na}_2\text{B}_4\text{O}_7$ buffer solution with electrode A. The E/t program applied considered a first potential step at -1.2 V for 10 min. During this lapse of time sodium sulfide was added to reach 5 mM hydrosulfide ion concentration. Further potential steps were applied in the potential range between -0.9 and -0.6 V, and thin films of Cu_xS were obtained (electrode B). For electrode B, the charge involved in the electroformation of a Cu_xS phase increased linearly with the number of spin-coating applications (sca) with a slope close to 0.3 $\text{mC cm}^{-2} \text{ sca}^{-1}$. For all electrochemical experiments an ITO/ Cu_xS electrode, involving an anodic charge of 0.5 mC cm^{-2} , was employed (1–2 sca). EIS study in potentiostatic mode was performed with electrode B (formed at -0.7 V according to the procedure above-described) in 0.05 M $\text{Na}_2\text{B}_4\text{O}_7$ buffer solution containing 5 mM hydrosulfide ion concentration. During EIS, a 5 mV rms ac signal with a frequency range from 100 kHz to 10 mHz was applied. The electrode was polarized in the potential range -0.6 to -0.9 V. All the electrochemical experiments were carried out with a Zahner IM6e potentiostat/galvanostat. The data acquisition and data analysis were performed using a THALES package from Zahner Elektrik GmbH & Co.

Photovoltammetric measurements with electrode B was performed with a PAR model 263 potentiostat connected to a PAR model 5210 two-channel lock-in analyzer. The incident light from a 50 W halogen lamp source was chopped at 30 Hz. Photovoltammograms in the -0.6 to -1.2 V range were scanned in the negative going potential sweep at a scan rate of 0.002 V s^{-1} in an electrolytic solution of 0.05 M $\text{Na}_2\text{B}_4\text{O}_7$ that contains 5 mM hydrosulfide ion concentration.

Morphology studies of electrodes were realized ex situ with a Nanoscope IIIa (Digital Instruments, Santa Barbara, CA) using tapping mode. EDAX study of electrode B was performed with a JEOL 5410 scanning electron microscope with an EDAX microprobe. Optical absorbance spectra of this electrode were obtained on a Hewlett-Packard 8452-A diode-array spectrophotometer. AFM and optical absorbance experiments were performed with electrodes ITO/Cu and ITO/ Cu_xS , obtained with 5 sca. For EDAX analysis ITO/ Cu_xS electrodes involving an anodic charge of 8.3 mC cm^{-2} were employed.

Results and Discussion

Voltammetric Study. Figure 1 shows the voltammetric profiles for the systems ITO, ITO/Cu (electrode A) in 50 mM borate buffer solution, pH 9.2, in the presence and absence of sodium sulfide. In the potential range studied (-1.2 to 0 V) no electrochemical processes were observed on the ITO electrode (profile 1). For electrode A in the absence of sulfide ion, in the positive-going potential scan the current increases due to the electroformation of cuprous oxide. In the negative-going potential scan the cathodic current peak located at the potential of -0.32 V

(11) Anuar, K.; Zainal, Z.; Hussein, M. Z.; Ismail, H. *J. Mater. Sci.: Mater. Electron.* **2001**, *12*, 147.

(12) Mastai, Y.; Gla, D.; Hodes, G. *J. Electrochem. Soc.* **2000**, *147*, 1435.

(13) Avey, A. A.; Hill, R. H. *J. Am. Chem. Soc.* **1996**, *118*, 237.

(14) Tejos, M. Doctoral Thesis, Universidad Católica de Valparaíso, Chile, 1999.

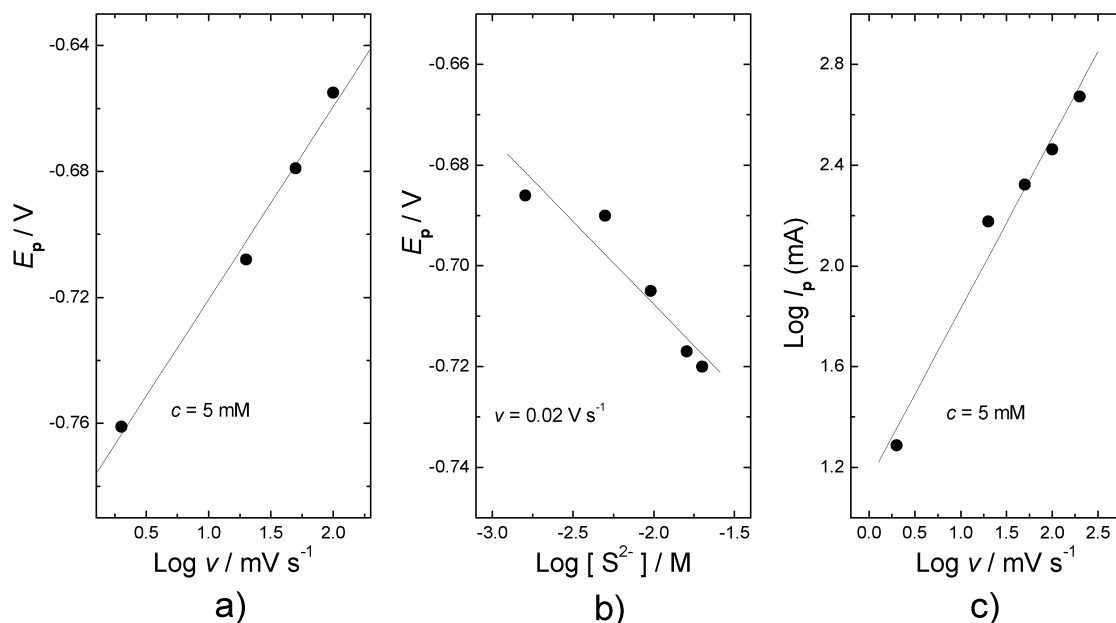


Figure 2. Potentiodynamic parameters related to the Cu_xS formation: (a) peak potential variation as a function of the logarithm scan rate; (b) peak potential variation as a function of the logarithm of the sulfide molar concentration; (c) variation of the anodic current peak as a function of the scan rate.

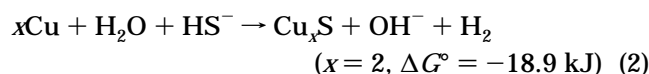
is attributed to the electroreduction of the cuprous oxide previously formed. The anodic and cathodic processes previously described are in accordance with previously reported results for copper oxides in alkaline media.^{1,2,4,5,15} This process can be represented through eq 1.



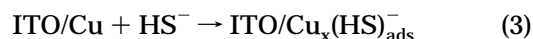
To study the formation of Cu_xS without the interference of copper oxides, electrode A was polarized at -1.0 V for 10 min, followed of the addition of Na₂S until reaching a 5 mM formal concentration. The electrode was maintained at -1.0 V for an additional 10 min, and then the potential was scanned in the anodic direction. A well-defined anodic current peak is observed at -0.7 V; the charge involved was close to 0.6 mC cm^{-2} . Other authors⁴ observe a prepeak attributed to the UPD of hydrosulfide layer on the copper surface which was not observed in the conditions of the present work; then the only peak observed is assigned to the copper sulfide formation.

In the negative potential sweep starting from -0.6 V, only a cathodic maximum current peak located at -1.05 V is observed, which corresponds to the cuprous sulfide reduction. No prepeak attributed by other authors^{2,4} to either the cupric sulfide reduction or nonstoichiometric compound (Cu_{2-x}S) reduction was observed in these experiments. The ΔE_p magnitude clearly indicates that the process of electroformation, and electroreduction of a Cu_xS phase is irreversible.

The Q_a/Q_c charge ratio corresponding to the first potentiodynamic cycle was lower than 1, showing that during the negative going potential scan takes place both, the reduction of cuprous sulfide electrochemically formed in the positive going potential scan and the cuprous sulfide chemically formed in a pathway that occurs in parallel with the electrochemically process according to the following reaction:



Nevertheless, when the electrode is successively cycled, the Q_a/Q_c charge ratio is close to 1. The linear variation of the anodic current peak (E_{pa}) with scan rate (v) and sulfide concentration (c) is shown in Figure 2. The slope are close to $1.15RT/\alpha F$ ($\alpha = 0.5$) per decade of v and to $-2.303RT/nF$ ($n = 2$) per decade of c . These values indicate that electroformation of a Cu_xS phase is controlled by the first electron transfer, and the total number of electrons involved in the process is close to 2. The effect of the scan rate on the anodic current peak is shown in Figure 2C. A linear relationship of current maximum with $v^{1/2}$ reveals the existence of a totally irreversible diffusion-controlled process. According to the above potentiodynamic parameters, the following sequence of reaction can be proposed for the electroformation of a Cu_xS phase:



To estimate the stoichiometry of the Cu_xS phase potentiodynamically formed, we have considered the following relation proposed by Delahay.¹⁶

$$E_{pa} = E^\circ + \frac{0.0218}{n} - \frac{0.059}{n} \log[S^{2-}] \quad (6)$$

In this relation, E_{pa} is the potential current peak and E° represents the standard potential of a half cell Cu/Cu₂S/S²⁻. According to the present results, E° was -0.83 V vs Ag/AgCl for the Cu_xS formed phase in the 0.05 M Na₂B₄O₇ buffer solution containing sulfide ion. This potential value lies in the potential range $-1.2 \text{ V} < E^\circ < -0.73 \text{ V}$ vs. Ag/AgCl reference electrode estimated by Sato for the

(15) Collisi, U.; Strehblow, H.-H. *J. Electroanal. Chem.* **1990**, *284*, 385.

(16) Delahay, P. *New Instrumental Methods in Electrochemistry*; Interscience: New York, 1954; p 124.

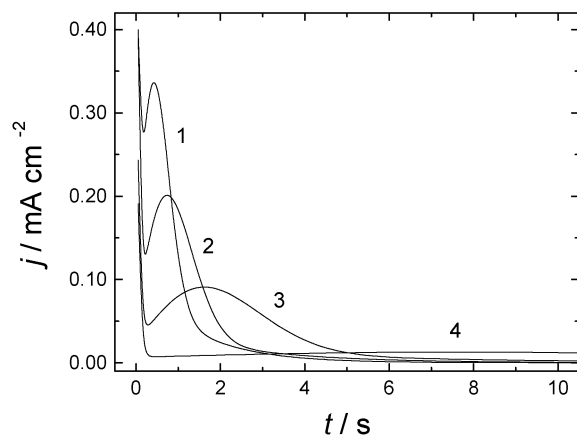


Figure 3. j/t transients obtained with electrode A in 0.05 M $\text{Na}_2\text{B}_4\text{O}_7$ + 5 mM Na_2S solution at different potentials: (1) -0.750 V, (2) -0.775 V, (3) -0.800 V, (4) -0.825 V. Electrode area = 1 cm^2 .

existence of a thermodynamically stable phase of Cu_2S .¹⁷ On the other hand, the polarization of electrode A for 20 min at the potential of the anodic current peak in a sulfide containing solution allowed to obtain an interface whose potential value measured against Cu/CuSO_4 50 mM, K_2SO_4 100 mM, pH 2.0 reference electrode (0.029 V vs Ag/AgCl) was 0.136 V. This means that in these last conditions the Cu_xS phase present, during the measurement, corresponds to a nonstoichiometric copper sulfide with $x = 1.9615$.⁹ The x value difference in the copper sulfide film under the Sato' consideration and the last experiment results would be attributed to the instability of the Cu_xS phase, which occurs when the circuit had to be opened in order to measure the potential of the interface against the Cu/CuSO_4 50 mM, K_2SO_4 100 mM, pH 2.0 reference electrode. As a matter of fact, when an electrode B was formed at a potential of -0.7 V, in the presence of sulfide ion, and then the circuit was open, the potential of the interface evolves toward positive values (-0.34 V) and nonstoichiometric phases of Cu_xS ($x < 2$) are obtained. From this potential they can be reduced in the -0.5 to -0.8 V potential range when a negative-going potential scan (0.02 V s^{-1}) is applied. (These facts are not shown in the figures.)

Current Transients Study. Figure 3 shows various $j-t$ responses for potentiostatic pulses corresponding to different overpotentials applied to electrode A in a sulfide-containing solution. The electrode was initially polarized at -1.10 V for 20 min in order to avoid any surface oxidation and then stepped to an E_s value in the $-0.8 \text{ V} < E_s < -0.6 \text{ V}$ range. The general shape of the $j-t$ transient is characteristic of a nucleation and growth process. At very short times ($t < 1$ s) a double-layer charging takes place, and then an increase of current is observed due to the formation and growth of Cu_xS nuclei. The current rises to reach a maximum and finally decreases until reaching a stationary negative current value. Transient currents obtained at potentials more negative than -0.8 V do not show current maximum, and only a current due to a double-layer charging is appreciated.

The current at times longer than 10 s attains a stationary negative current values for all potentials studied (-1 to $-4 \mu\text{A cm}^{-2}$). This aspect differs from previous works performed on polycrystalline copper electrodes involving electric charges greater than those used in this work and where positive stationary current

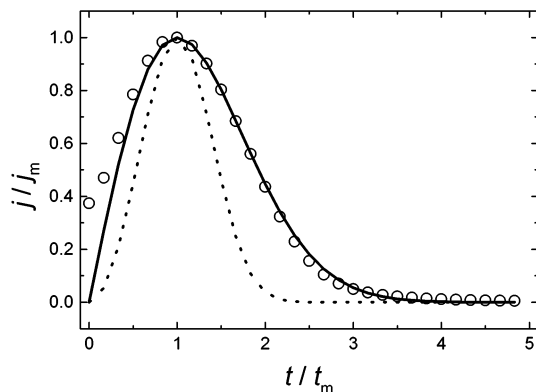


Figure 4. Nondimensional j/j_m vs t/t_m plots for the nucleation of Cu_xS obtained from j/t transient at -0.775 V: (continuous line) instantaneous; (dotted line) progressive, (○) experimental data.

values were obtained.^{2,5} Under the experimental conditions employed (inert atmosphere, absent of oxygen, and other oxidant species), we attribute this current to the water reduction that simultaneously takes place with the electroformation of the copper sulfide film Cu_xS . To obtain corrected $j-t$ transients that consider only the electroformation of Cu_xS and not this side process and also to obtain information about the nucleation and growth mechanism of the Cu_xS phase, expression 7 was employed, at each potential value studied, for subtract the current density attributed to the water reduction from each $j-t$ transients:

$$j = -a(1 - \exp(-bt^2)) \quad (7)$$

In this expression we postulate that water reduction follows an exponential law with time. Under this assumption, a constant current density value is attained when $t \rightarrow \infty$. In the above expression, j is the current density related to water reduction, t is the time considered, and a and b are constants that depend on the potential applied. They were evaluated by a nonlinear fit procedure.

Figure 4 shows a corrected $j-t$ transient obtained at -0.775 V in a dimensionless graph from which the nucleation behavior can be evaluated by comparison with the theoretical plots for the limiting nucleation cases, i.e., progressive or instantaneous.¹⁸ Except at very short times where the double-layer charging is occurring results fit exactly with an instantaneous bidimensional nucleation mechanism (continuous line). This behavior (IN2D) explains that the current reach a zero value at longer times because the number of copper sites for the sulfidization is limited.

Figure 5 shows a corrected transient $j-t$ which was deconvoluted in three current density contributions: j_{DL} , j_{I} , and j_{II} . j_{DL} represent the current density attributed to the double-layer charging and is given by an expression of the form¹⁹

$$j_{\text{DL}} = A \exp\left(-\frac{t}{B}\right) \quad (8)$$

where $A = \Delta V/R$ and $B = RC$. ΔV is the amplitude of

(17) Sato, M. *Electrochim. Acta* **1966**, *11*, 361.

(18) Southampton Electrochemistry Group *Instrumental Methods in Electrochemistry*; Ellis Horwood: Chichester, 1985; Chapter 3.

(19) Beaunier, L.; Cachet, H.; Froment, M.; Maurin, G. *J. Electrochem. Soc.* **2000**, *147*, 1835.

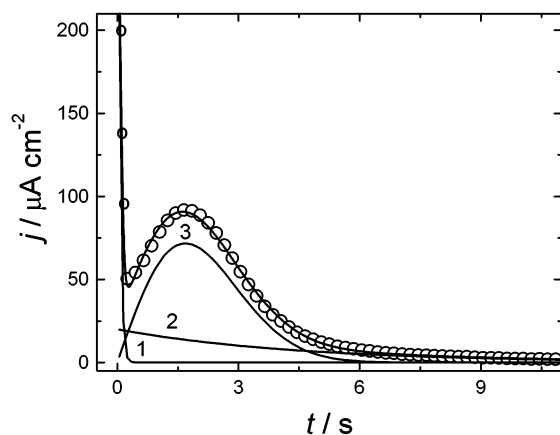


Figure 5. j/t transient obtained with electrode A in 0.05 M Na₂B₄O₇ + 5 mM Na₂S at the potential -0.775 V: (○) experimental curve, (—) fitted curve, individual contributions (1) j_{DL} , (2) j_i , (3) j_{II} .

the potential step, R is the resistance of the interface electrode/electrolyte, and C represents the capacity of the interface.¹⁹

The j_i contribution represents a current transient due to an instantaneous nucleation and circular bidimensional growth under diffusion control.² The instantaneous value of j_i is given by

$$j_i = E \exp(-Gt) \quad (9)$$

where $E = q\pi k_e D N_0$ and $G = \pi k_e D N_0$. D is the diffusion coefficient of the reacting species (HS^-), k_e is a proportionality constant, N_0 is the number of cluster sites for available nucleation at the surface, and q represents the charge density required for the sulfidization of the cluster sites.

Finally, the principal contribution of j_{II} represents the current density associated with an instantaneous bi-dimensional nucleation according to the following expression¹⁸

$$j_{II} = Ht \exp(-Lt^2) \quad (10)$$

where $H = 2\pi F M h N_0 K \rho^{-1}$ and $L = \pi N_0 K^2 M^2 \rho^{-2}$. F is the Faraday constant, M is the molecular weight, N_0 and h are the number and the height of the cluster sites, respectively, K is the rate of the nucleation process, and ρ is the density of the growing compound. The same behavior was observed in the current transient obtained at other potential values studied.

The presence of two types of nucleation and growth mechanisms (j_i and j_{II}) in the transients can be explained considering the model represented in Figure 6. In this model two sites of copper for the sulfidization process are considered: The first one with adsorbed hydrosulfide ions and responsible for the process IN2D under charge-transfer control (j_{II}). The other one, without adsorbed hydrosulfide ion, is affected by the diffusion of the hydrosulfide ions from solution and is responsible for the process IN2D under diffusional control (j_i).

Precedent discussion considers the existence of a stationary negative current observed during the sulfidization of a copper thin film under potentiostatic conditions which was attributed to the simultaneous water reduction. Under identical conditions, a bare ITO electrode shows always a stationary negative current, which was lower than the observed on ITO/Cu_xS electrode. Besides, on an ITO/Cu_xS electrode, an important increase of the

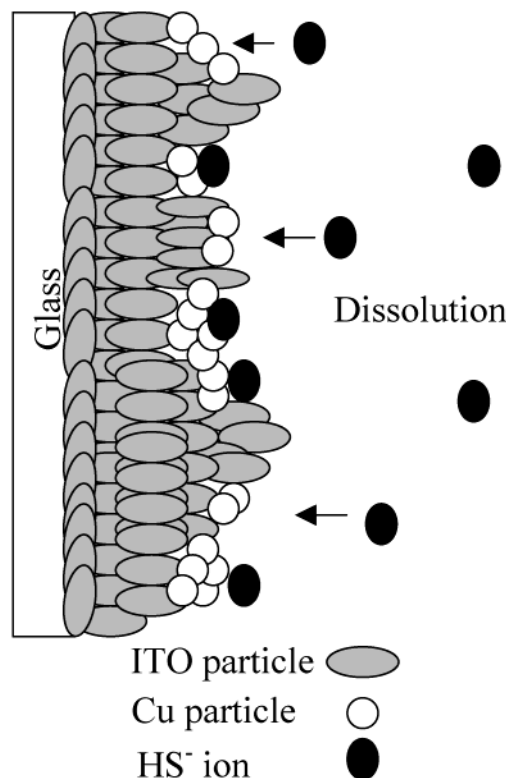
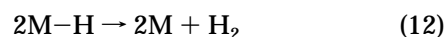
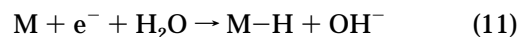


Figure 6. Model representing the Cu_xS nucleation and growth mechanism at electrode A in 0.05 M Na₂B₄O₇ + 5 mM Na₂S.

stationary negative current value was observed under illumination (ca. 70%). These experimental results can be explained considering that the water reduction would be occurring on different sites presents on the electrode such as ITO/Cu_xS and bare ITO.

The general scheme for the water reduction on a substrate can be considered as follows:^{20,21}



where M represents a substrate site and M-H hydrogen adatoms.

To gain insight into this reaction, which is important because it appears responsible for the spontaneous chemical formation of Cu_xS (eq 2) and of the presence of a negative current density that appears during the potentiostatic electroformation of the Cu_xS phase, an electrochemical impedance study was carried out on ITO and ITO/Cu_xS electrodes. Figure 7 shows Nyquist diagrams for both electrodes recorded at -0.6 and -0.9 V. Both electrodes showed a capacitive response, and at any frequency, the total impedance (Z_T) was lower for the Cu_xS electrode than the ITO electrode. This fact is in concordance with the above describe experiments that showed that the stationary current density measured on ITO/Cu_xS is higher than ITO. Besides, these results show that the nature of electrode surface has an important effect in the water reduction.

(20) Barber, J. H.; Conway, B. E. *J. Electroanal. Chem.* **1999**, 461, 80.

(21) Bockris, J. O. M.; Khan, S. U. M. *Surface Electrochemistry, A Molecular Approach*; Plenum Press: New York, 1993; pp 310–316.

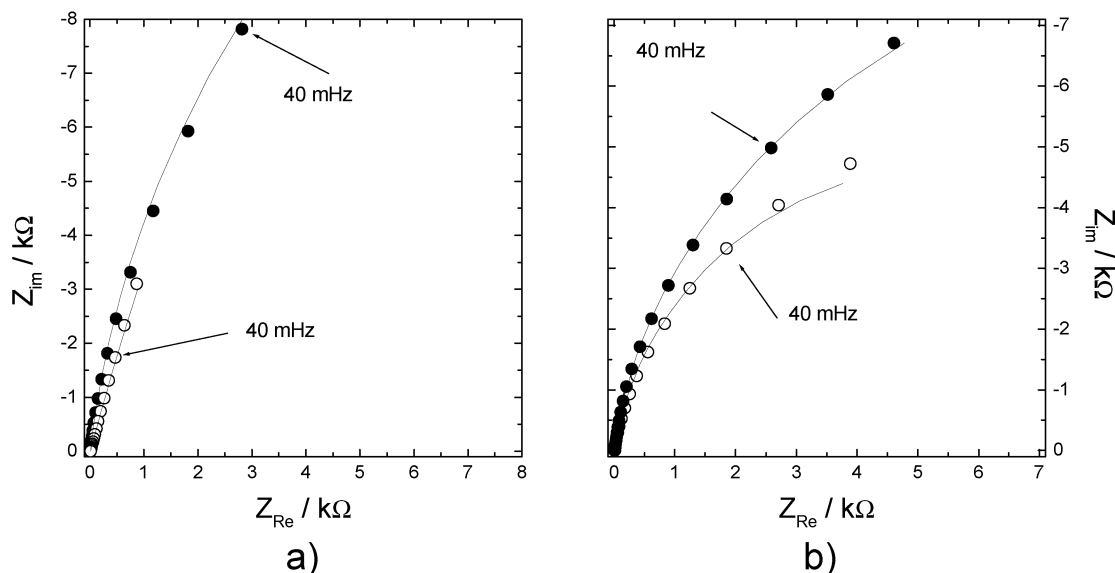


Figure 7. Nyquist diagrams for ITO and ITO/Cu_xS electrodes in 0.05 M Na₂B₄O₇ + 5 mM Na₂S: (a) -0.60 V, (b) -0.90 V; (●) experimental data for ITO electrode, (○) experimental data for ITO/Cu_xS electrode; (—) fitted data with transfer function (14).

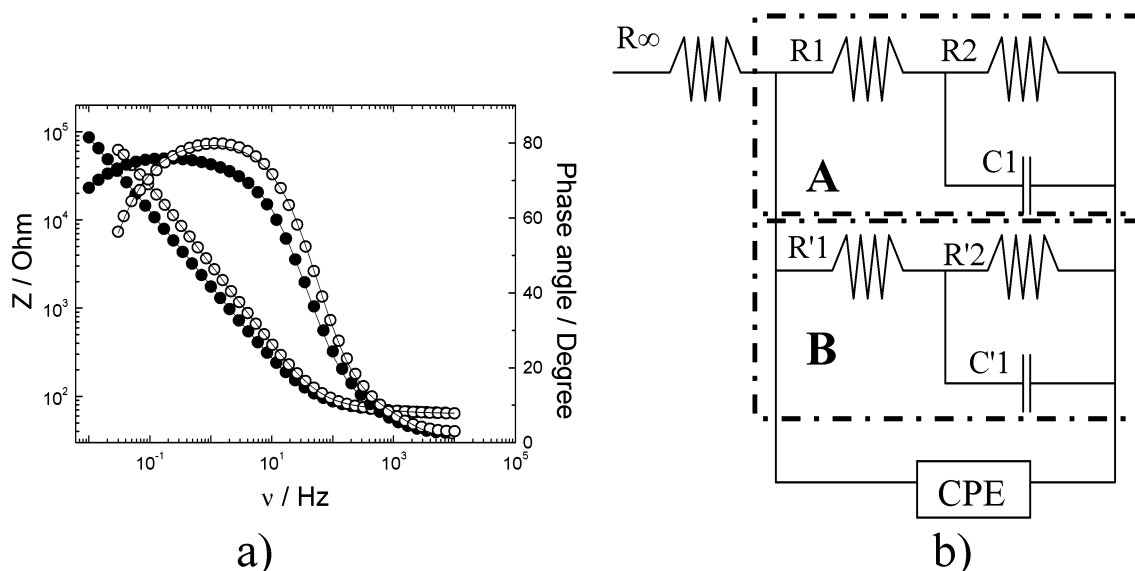


Figure 8. (a) Bode plots for ITO/Cu_xS electrode in 0.05 M Na₂B₄O₇ + 5 mM Na₂S. Experimental data at the potentials (●) -0.60 V and (○) -0.90 V, (—) fitted data with transfer function (15). (b) Equivalent circuit representing the transfer function (15).

Experimental data were analyzed using a nonlinear fit according to the following expression:

$$Z_T = R_\infty + Z_{TF} \quad (14)$$

$$Z_{TF} = \left[\frac{1}{(R_1 A)^{-1} + R_2 + i\omega C_1 A^{-1}} + \frac{1}{(R'_1 B)^{-1} + R'_2 + i\omega C'_1 B^{-1}} + (i\omega C_2)^\alpha \right]^{-1} \quad (15)$$

$$A = \frac{1}{R_1^2} + \omega^2 C_1^2 \quad (16)$$

$$B = \frac{1}{R_1'^2} + \omega^2 C_1'^2 \quad (17)$$

where $\omega = 2\pi f$ and R_∞ denotes the ohmic resistance of the system. Z_{TF} is the transfer function of the system that

contains the terms A and B , which are similar because they represent the occurrence of the same process but at surfaces that differ in nature. R_1 and R'_1 are the reaction resistance for pathway 11. C_1 and C'_1 are the capacitances due to the existence of hydrogen adatoms formed in this pathway. R_2 and R'_2 are reaction resistance for the pathway 13.

Figure 8 shows experimental and simulated Bode diagrams for the ITO/Cu_xS electrode obtained at the potentials -0.60 and -0.90 V and in the insert the proposed equivalent circuit representing the transfer function above-described. Good concordance between the experimental and simulated data can be appreciated. In the equivalent circuit, the systems denoted as A and B represent the water reduction occurring on Cu_xS phase and bare ITO, respectively. Table 1 shows values of different contributions to the total impedance. In both systems, R_1 and R'_1 values are higher than R_2 and R'_2 values, respectively, showing that the water reduction process is controlled by the first charge transfer that leads

Table 1. Equivalent Circuit Parameters for Electrode B in 0.05 M Na₂B₄O₇ + 5 mM Na₂S at Different Applied Potentials

<i>E</i> /V	system A			system B			CPE		
	<i>R</i> ₁ /kΩ	<i>C</i> ₁ /μF	<i>R</i> ₂ /kΩ	<i>R</i> ₁ '/kΩ	<i>C</i> ₁ '/μF	<i>R</i> ₂ '/kΩ	<i>C</i> ₂ /μF	α	<i>R</i> _∞ /Ω
−0.6	3170	13.36	479.6	3050	3.6	51.08	35.62	0.825	106.0
−0.7	1310	12	307	1220	1.33	35.0	28.87	0.930	110.0
−0.8	511	9.82	292.1	477.8	0.98	16.87	23.43	0.917	111.6
−0.9	349.8	9.59	282	327.8	0.94	12.24	22.68	0.901	111.7

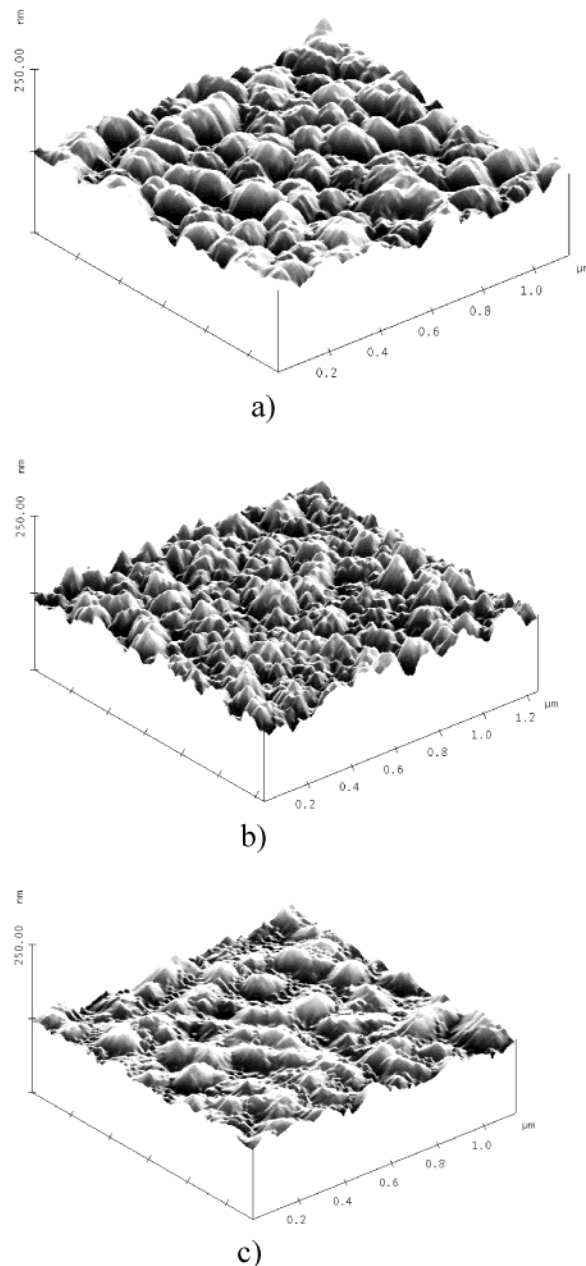
to the hydrogen adatoms formation. When the potential is made more negative, *R*₁, *R*₁', *C*₁, and *C*₁' values decrease, indicating that the rate of the pathway 11 prevails and consequently a lower coverage for hydrogen adatoms is achieved. In this work *C*₁' is attributed to the capacitance of hydrogen adatoms present on uncovered ITO sites. This assumption is supported because in a parallel experiment performed in the same experimental conditions with an ITO electrode, the capacitance measured (3 μF cm^{−2}) was close to the *C*₁' value that appears in Table 1.

From these results it is possible to conclude that water reduction process takes place at both types of surfaces present in the electrode, but its extent is greater on the Cu_xS phase than bare ITO. Similarly, these results would explain the increase of the stationary negative current when an ITO/Cu_xS electrode was illuminated (see above) due to the p-character of the Cu_xS semiconductor. Because the existence of two redox complementary processes, they also explain the instability of the Cu_xS phase that is observed at open circuit in aqueous solutions.

Morphology Study of the Cu_xS Phase by AFM.

Figure 9 shows 3D AFM images of the surfaces of ITO, ITO/Cu, and ITO/Cu_xS electrodes; for both last electrodes 5 sca was necessary apply in order to obtain well-defined AFM images. Figure 9a shows a granular morphology of the ITO surface; the average particle diameter is close to 135 nm. Electrode A (Figure 9b) shows deposits of copper and/or copper-containing oxygen particles which are preferentially located in the valleys delimited by ITO particles. This form of deposit seems to be characteristic of the spin-coating technique employed, because during rotation the solution is freely moving between ITO particles. The average particle size found was close to 65 nm. The lowest average particle size present on the surface of electrode A, with respect to the observed on ITO, is due to the existence of Cu particles (in different forms) with particle diameter lower than 40 nm. Figure 9c shows the surface of an ITO/Cu_xS electrode. It is observed that the shape of the deposit is similar to that observed in electrode A and that the average particle diameter is close to 62 nm. Nevertheless, particles of Cu_xS with diameter lower than 20 nm can be observed in some regions of the surface. Like the electrode ITO/Cu, the particles of the Cu_xS compound appear deposited preferentially in the valleys.

Nevertheless, the possibility that an extremely thin film of Cu_xS covering ITO particles is not rejected. Under this assumption Cu deposits would be present either on the top of the ITO particles or in the valleys left by them. This picture would explain also the existence of two different sites disposable for nucleation and growth of a Cu_xS phase. As a matter of fact, when a linear EDAX analysis realized on an electrode ITO/Cu_xS (8.3 mC cm^{−2} anodic charge) and covering a distance over 15 μm, Cu and S signals appear in the whole trajectory of the probe, and an average Cu/S ratio of 2.05 ± 1.50 was found. On the other hand, when an EDAX analysis covering the whole surface of the electrode is realized, besides of the signal of the elements constituents of the ITO substrate, Cu and S signals (1.7 and 0.77 atom %, respectively) were appreci-

**Figure 9.** AFM images for (a) ITO surface electrode, (b) ITO/Cu surface electrode, and (c) ITO/Cu_xS surface electrode.

ated. From these figures, a Cu/S ratio of 2.2 ± 0.1 was estimated, indicating a lightly copper excess. The apparent contradiction of these values with the corresponding *x* values (*x* < 2) derived from the electrochemical experiences can be explained taking in account that the optical and electrochemical techniques employed give information that depend of the depth of the sample analyzed. Figure 10 shows the UV-vis spectra of the sample ITO/Cu_xS obtained after 5 sca. Figure 11 plots (*A*hν)^{0.5} vs *hν*; the data were obtained from Figure 10 and

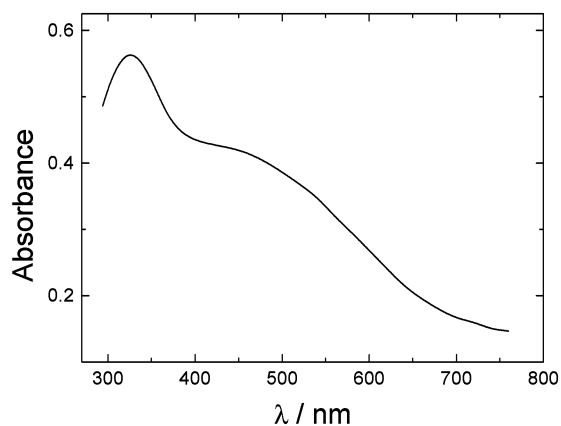


Figure 10. UV-vis spectra of electrode ITO/Cu_xS with ITO electrode as blank.

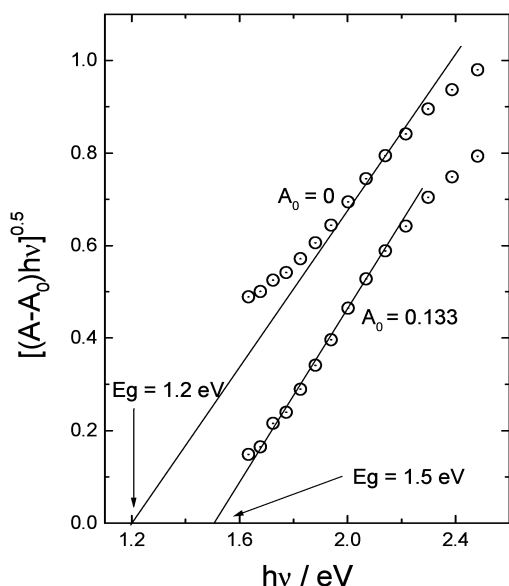


Figure 11. $[(A - A_0) h\nu]^{0.5}$ vs $h\nu$ plot for ITO/Cu_xS electrode. Data obtained from Figure 10.

should yield a linear plot if the following expression is considered:³

$$A = A_0 + \frac{C(E - E_g)^{0.5}}{E} \quad (18)$$

where $E = h\nu$ is the photon energy, E_g is the band gap energy, and C is a constant, applied to indirect optical transitions. A_0 is a background absorbance due to a imperfect substrate compensation, sample reflectance, free carrier and impurity absorption, etc. Two values have been selected for A_0 , e.g., 0.0 and 0.133; the last one corresponds to the minimum absorbance of the sample. Band gaps of 1.2 and 1.5 eV were estimated for the A_0 values, respectively. The first value seems more correct and close to the 1.25 eV value previously reported for Cu_xS ($x \rightarrow 2$).²² Nevertheless, as has been previously assumed, the original value might lie between these E_g values considering the uncertainties involved in the measurements.³ A more reliable value would be obtained using photocurrent spectroscopy.

(22) Fahrenbruch, A. L.; Bube, R. H. *Fundamentals of Solar Cells*; Academic Press: New York, 1983; p 427.

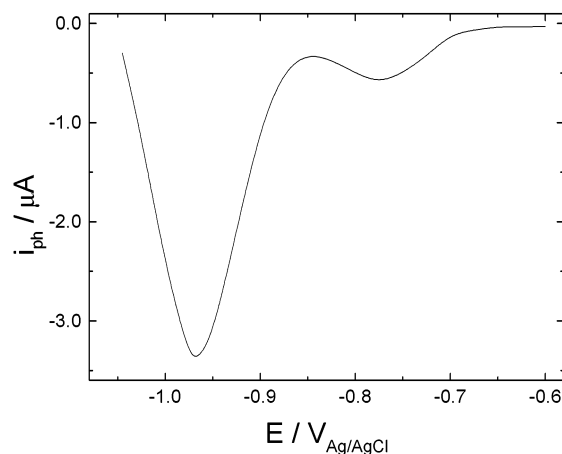


Figure 12. Photovoltammogram profile obtained with an ITO/Cu_xS electrode in 0.05 M Na₂B₄O₇ + 5 mM Na₂S. Negative going potential scan from -0.60 V was registered at 0.002 V s⁻¹.

Figure 12 shows the cyclic photovoltammogram recorded in a negative-going potential scan starting from a potential value of -0.6 V. The polarity of the photocurrent clearly indicates that the Cu_xS obtained is a p-type semiconductor. The principal photocurrent peak observed at a potential of -0.98 V corresponds to photoelectroreduction of copper sulfide film (compare with Figure 1). We attributed the smaller photocurrent peak observed at a potential close to -0.77 V to the photoelectroreduction of some non-stoichiometric copper sulfide compounds which were spontaneously formed during the setup of the experiment. The possibility that this photocurrent peak can correspond to copper oxide is rejected because such species are reduced at more positive potentials (-0.37 V). It is important to note that the photocurrent density values observed in the present work employing electrodes that contain thin film of Cu_xS ($x \rightarrow 2$) were always greater than the observed, in similar conditions (electrolyte, scan rate, illumination level), with those Cu₂S film electroobtained on polycrystalline copper substrate.¹ The differences observed can be related to a greater surface area present in the Cu_xS thin film, which in turn contains particles sized in the 20 nm range.

Conclusions

The sulfidization at -0.7 V of a thin film of copper disposed over ITO surface and obtained through the spin-coating technique allows to obtain, in borate buffer solution, pH 9.2, in the presence of 5 mM sodium sulfide, a Cu_xS phase with a stoichiometric factor (x) close to 2 with a particle size lower than 40 nm. In the experimental conditions assayed, it is probably that Cu_xS film cover only partially the ITO surface, and therefore, in the potential range where Cu_xS phase is stable, water reduction can take place onto both surface sites. The existence of both complementary redox processes would be responsible of the instability of the copper sulfide film observed when the electrical circuit is opened.

Acknowledgment. This work was funded by Fondecyt-Chile (Contract L.C. 8000022 and 3010016) and DGI-UCV. Financial support of Junta de Andalucía (Spain) is also gratefully acknowledged.

LA025711K